



LAWRENCE
LIVERMORE
NATIONAL
LABORATORY

Quantifying uncertainties of a Soil-Foundation Structure-Interaction System under Seismic Excitation

C. Tong

April 11, 2008

Disclaimer

This document was prepared as an account of work sponsored by an agency of the United States government. Neither the United States government nor Lawrence Livermore National Security, LLC, nor any of their employees makes any warranty, expressed or implied, or assumes any legal liability or responsibility for the accuracy, completeness, or usefulness of any information, apparatus, product, or process disclosed, or represents that its use would not infringe privately owned rights. Reference herein to any specific commercial product, process, or service by trade name, trademark, manufacturer, or otherwise does not necessarily constitute or imply its endorsement, recommendation, or favoring by the United States government or Lawrence Livermore National Security, LLC. The views and opinions of authors expressed herein do not necessarily state or reflect those of the United States government or Lawrence Livermore National Security, LLC, and shall not be used for advertising or product endorsement purposes.

This work performed under the auspices of the U.S. Department of Energy by Lawrence Livermore National Laboratory under Contract DE-AC52-07NA27344.

Quantifying Uncertainties of a Soil-Foundation Structure-Interaction System under Seismic Excitation *

Charles Tong
Center for Applied Scientific Computing
Lawrence Livermore National Laboratory
Livermore, CA 94550-0808

Abstract

We applied a spectrum of uncertainty quantification (UQ) techniques to the study of a two-dimensional soil-foundation-structure-interaction (2DSFSI) system (obtained from Professor Conte at UCSD) subjected to earthquake excitation. In the process we varied 19 uncertain parameters describing material properties of the structure and the soil. We present in detail the results for the different stages of our UQ analyses.

1 Problem Definition

The structure is two-story two-bay reinforced concrete frame. The foundations consist of reinforced concrete squat footings at the bottom of each column. The soil is a layered clay, with stiffness properties varying along the depth (see Figure 1, Courtesy of Professor Conte and Dr. Quan Gu at UCSD).

The frame consists of two stories each of height $h = 3.6m$ and $L = 20m$ across (horizontal direction). The columns are modeled using displacement-based Euler-Bernoulli frame elements with distributed plasticity, each with 4 Gauss-Legendre integration points. Foundation footings and soil layers are modeled through isoparametric four-node quadrilateral finite elements with bilinear displacement interpolation. The constitutive behavior of the steel reinforcement is modeled by using a one-dimensional J_2 plasticity model with both

*This work was performed under the auspices of the U.S. Department of Energy by Lawrence Livermore National Laboratory under Contract No. DE-AC52-07NA27344.

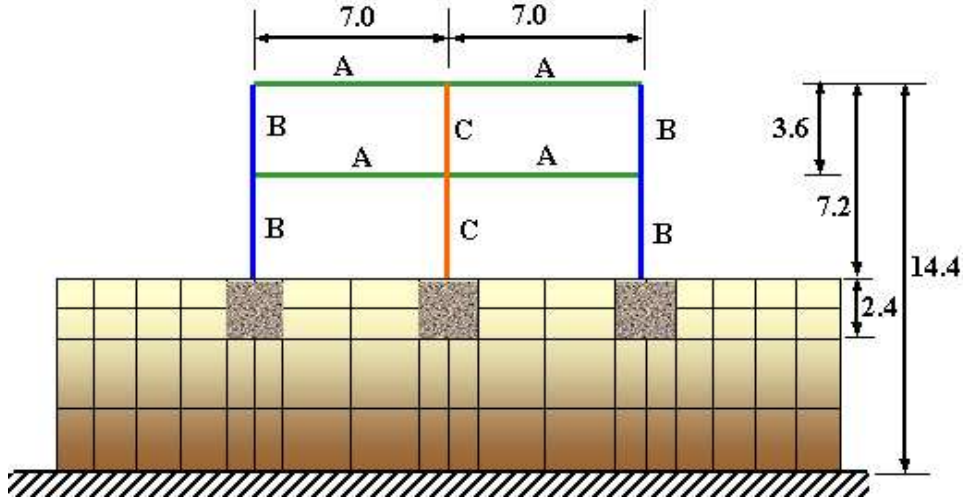


Figure 1: A 2D soil-foundation-structure-interaction system

kinematic and isotropic linear hardening. The concrete is modeled by using a Kent-Scott-Park model with zero tension stiffening. Different material parameters are used for confined (core) and unconfined (cover) concrete in the columns. The soil is modeled by using a pressure-independent multi-yield surface J_2 plasticity material model, specialized for plane strain analysis. Different material parameters are used for each of the four layers considered. The soil under a condition of simple shear has its bottom nodes fixed and the corresponding boundary nodes at same depth tied together. The node of the beam (3 degrees of freedom) and the corresponding node on the foundation concrete block (2 degrees of freedom), at the same location, are tied together in both the horizontal and vertical directions.

After static application of the gravity loads, the structure is subjected to a base excitation taken as three times the recorder data of the 1940 Elcentro earthquake, as shown in in Figure 2.

Uncertainties in the model parameters translate into uncertainties in the output responses of interest. In this report we study the effect of uncertainties in the soil and structure material parameters on the drift uncertainties under seismic excitation. The 19 material parameters are listed in Table 1 and the parameter correlations are given in Table 1. The parameters distributions are provided to us by Professor Conte and colleagues at UCSD.

The responses of interest in our study are:

inter-story drift ratios (IDR) : (Response 1 and 2) defined as

$$\text{IDR} = \frac{\text{maximum absolute inter-story drift}}{\text{story height}}$$

Roof drift ratio (RDR) : (Response 3) defined as

$$\text{RDR} = \frac{\text{max absolute X displacement at roof}}{\text{building height}}$$

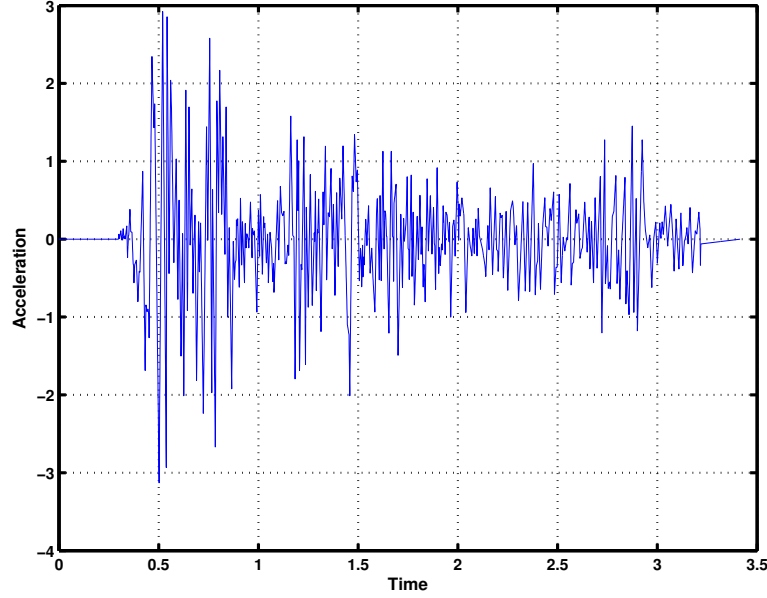


Figure 2: Fault component (3X) of 1940 Elcentro earthquake

Maximum floor acceleration (MFA): (response 4) computed by taking the second derivative of the horizontal displacement.

2 Introduction to Uncertainty Quantification

Uncertainty quantification (UQ) is a scientific discipline that conducts research and development of methodologies and mathematical methods to help

- Characterize the output uncertainties of a simulation model given parameter and model uncertainties (uncertainty assessment, forward propagation of uncertainties),
- Identify the major sources of uncertainties of a model (sensitivity analysis),
- Establish the integrity of a simulation model (validation),
- Tune a simulation model to match better with experiments (calibration),
- Assess the region of the validity of a simulation model (reliability/risk analysis),
- Provide information on which additional experiments are, needed to improve the understanding of a model,

and others.

To accomplish the goals of UQ, many computer experiment design and analysis tools are needed. In this section we describe a few mathematical/statistical tools for UQ, with primary

Table 1: **Material parameters**

	Parameter	Distribution	Mean	standard deviation
Upper Cover Concrete	f_c	Lognormal	27588.5	0.2 * Mean
	e_{c0}	Lognormal	0.002	0.2 * Mean
	e_{cu}	Lognormal	0.008	0.2 * Mean
Upper Core Concrete	f_c	Lognormal	34485.6	0.2 * Mean
	f_{cu}	Lognormal	20691.4	0.2 * Mean
	e_{c0}	Lognormal	0.004	0.2 * Mean
	e_{cu}	Lognormal	0.014	0.2 * Mean
Upper	E	Lognormal	2.0e8	0.033 * Mean
Steel	S_y	Lognormal	248200	0.106 * Mean
	Hkin	Lognormal	1.613	0.2 * Mean
Foundation	E	Lognormal	2.0e7	0.2 * Mean
Soil Layer #1	G	Lognormal	54450	0.3 * Mean
	τ_{\max}	Lognormal	33.0	0.25 * Mean
Soil Layer #2	G	Lognormal	33800	0.3 * Mean
	τ_{\max}	Lognormal	26.0	0.25 * Mean
Soil Layer #3	G	Lognormal	61250	0.3 * Mean
	τ_{\max}	Lognormal	35.0	0.25 * Mean
Soil Layer #4	G	Lognormal	96800	0.3 * Mean
	τ_{\max}	Lognormal	44.0	0.25 * Mean

Table 2: **Material parameter correlations**

Parameter	Parameter	Correlation
f_c (core)	f_c (cover)	0.8
E_{c0} (core)	E_{c0} (cover)	0.8
E_{cu} (core)	E_{cu} (cover)	0.8
E_{c0} (core)	E_{c0} (core)	0.8
f_c (core)	f_{cu} (core)	0.8
E_{c0} (cover)	E_{cu} (cover)	0.8
E_{c0} (core)	E_{cu} (cover)	0.64
E_{cu} (core)	E_{c0} (cover)	0.64
f_{cu} (core)	f_c (cover)	0.64
G (# 1)	τ_{\max} (# 1)	0.4
G (# 2)	τ_{\max} (# 2)	0.4
G (# 3)	τ_{\max} (# 3)	0.4
G (# 4)	τ_{\max} (# 4)	0.4
τ_{\max} (# 1)	τ_{\max} (# 2)	0.4
τ_{\max} (# 2)	τ_{\max} (# 3)	0.4
τ_{\max} (# 3)	τ_{\max} (# 4)	0.4

focus on the sampling-based or non-intrusive techniques for global sensitivity analysis and failure analysis.

Prior to performing any uncertainty sensitivity analysis on a model, much diligence is required to compile a detailed model specification, since results concluded from the analysis are valid only with respect to the given model specification. The specification may include the model geometry, code version, input parameters (for example, material strength parameters), algorithmic parameters (for example, the grid resolution or convergence tolerances), simulation output responses, and any other assumptions about the model.

2.1 Global Sensitivity Analysis

Global SA analysis studies the effects of the variations of inputs on the model outputs in the allowable ranges of the input space. Saltelli *et al.* [8] have defined global methods by two properties:

1. The inclusion of influence of scales and shapes of the probability density functions for all inputs.
2. The sensitivity estimates of individual inputs are evaluated while varying all other inputs (multi-dimensional averaging).

A common method for measuring sensitivities is variance decomposition which apportions the total output variance to each individual input. For high dimensional (large number of uncertain inputs) models, several approaches can be useful: (1) make linearity or monotonicity assumptions about the model output behavior and apply classical regression analysis; (2) create an approximate response function directly on the high dimensional problem and perform variance decomposition on it; and (3) perform screening to identify a subset of the most important inputs, create an response function for the lower dimensional problem and apply variance decomposition.

The rationale for approach (2) is that if most of the input parameters have negligible effect on the output, a high-dimensional response function is almost as good as the response function for the down-selected set of inputs, provided that a good sampling design is used (The unimportant parameters amount to introducing noises to a lower dimensional problem). This approach often uses Gaussian process-based Bayesian methods. The rationale for approach (3) is that when there is a lack of prior information on the output behavior, it makes sense to perform a qualitative analysis followed by a quantitative analysis on the reduced (smaller number of parameters) problem. We will introduce these approaches in the following.

2.1.1 Regression-based Sensitivity Analysis

Regression analysis concerns developing a mathematical model relating the inputs and model outputs, and then evaluate how good the model is. Strictly speaking, regression analysis is

not statistical in nature, since it involves only numerical linear algebra. Both linear and nonlinear regression analyses have found widespread uses in applications. As a result of linear regression analysis, a quantity called standardized regression coefficients (SRCs) can be computed. When the inputs are independent and the model is linear, the absolute value of the SRCs can be used as a measure of importance. To verify that linear regression provides acceptable fitting of data, the fitting errors should be carefully analyzed. The fitting is considered to be acceptable if the error distribution is Gaussian-like with small standard deviation. A quantity called adjusted R^2 can also be used to judge the quality of linear fit.

SRCs are poor indicators when the underlying relationships are nonlinear. However, if the relationships are monotonic, the rank transformation can be used to linearize the input-output relationships. In rank transformation, the smallest value of each variable is given a rank of 1, and equal values are given averaged ranks. The regression analysis applied to the rank-transformed data yields the standardized ranked regression coefficients (SRRCs), which measure the strength of monotonic relationship between the variables. Random and quasi-random samples can be used to compute the SRCs and SRRCs.

2.1.2 Bayesian Sensitivity Analysis

In [6], Bayesian inferences has been advocated as a viable approach to analyzing sensitivities. In this scenario the model is considered as an unknown function until it has been evaluated given a design point. The approach begins with an assumed prior distribution for the model. This prior distribution is subsequently updated using sampling together with the Bayesian paradigm. This gives a posterior distribution which can be used to make inferences about the sensitivity measures. A popular prior distribution is in the form of a Gaussian process (GP). A key requirement to use Gaussian processes is that the model is a smooth function of its input (uncertain) parameters.

A GP model is determined by its mean and covariance functions. The mean can be defined by specifying the regressor functions (to express prior beliefs about input-output relationships) as well as the corresponding weights (say β , which is a vector) . The covariance function, in the simplest case, can be represented by a correlation function (to express prior beliefs about the smoothness of the model output) and a few other parameters (called hyperparameters). Thus, the Bayesian approach has the advantage that the associated GP allows for incorporation of uncertainties via the hyperparameters. To estimate these hyperparameters, the model has to be run on a carefully selected set of sample points which should be selected to give good information about the model behavior over the parameter space. In practice, when little is known about the model behavior over the parameter space, a space-filling space should be used. The detailed mathematics of forming the GP can be found in [6].

GP-based sensitivity analysis can be applied directly to a high dimensional model without the multiple steps as described next, provided that the model output is a sufficiently smooth function of its inputs and the number of important parameters is a small percentage of the

total number of parameters while all unimportant parameters have negligible effects. For high-dimensional models with unknown smoothness, we strongly recommend using multi-stage (to be described next) Bayesian sensitivity analysis, i.e. use GP-based screening for parameter down-select and then GP-based variance decomposition on the subset of important parameters.

GP-based methods do have the disadvantages that the estimation of the hyperparameters can be difficult and computationally expensive for large sample size. In addition, a requirement for the GP algorithms to work is that the covariance matrices created in the optimization stage are positive definite (all eigenvalues greater than zero). Based on our limited experience, many GP algorithms do frequently encounter indefinite covariance matrices at the internal optimization steps. Remedies such as inexact decomposition of the covariance matrices have been proposed although not much is known about their effect on the results.

In Bayesian framework, GP-based methods are not the only methods available. Artificial neural network (ANN), multivariate splines and support vector machine (SVM) can also be considered as Bayesian method since the kernel in this methods can be viewed as prior information and their coefficients are posterior information derived from the sample data.

2.1.3 Multi-step Sensitivity Analysis

Multi-step sensitivity analysis has been proposed and applied in several applications [8, 9]. A multi-step SA comprises a four-step process for high dimensional models.

1. Construct a complete description of the input parameters (that is, the ranges and forms of the distributions).
2. If the number of uncertain input parameters is relatively small (say, less than 10), skip to Step (3). Otherwise, perform a down-select screening analysis on all uncertain parameters. There are several alternatives to the choice of screening methods. We recommend using two or more screening methods to confirm the results.
3. If the simulation is computationally intensive and the output response is a “relatively” smooth function of the uncertain inputs, we should consider using response surfaces (other names are: surrogate functions, emulators) to construct approximate models.
4. Perform a quantitative sensitivity analysis via variance decomposition techniques.

Step (2) above is a coarse sensitivity analysis seeking to identify qualitatively a subset of the most sensitive parameters. If there is no prior knowledge of the smoothness of the function output, this coarse analysis may incur errors, which may be classified as Type I or Type II. Type I errors occur when the analysis mistakenly identifies unimportant parameters as important ones. Type II errors, which is more serious, results when important parameters are identified as unimportant ones. It is therefore recommended (also by Oakley and Hagan

[6]) that, rather than relying on just one single screening approach, multiple measures are used in this step.

2.2 The Morris Screening Method

The Morris method is an effective screening method for large number of uncertain parameters. To generate the Morris design, a base sample point $X^{(1)}$ is created such that each of the M (M is the number of input parameters) components of $X^{(1)}$ is randomly selected from the set $\{0, 1/(p-1), 2/(p-1), \dots, 1\}$, where p is a pre-selected integer (for example, $p = 4$). The second sample point $X^{(2)}$ is created from $X^{(1)}$ by perturbing one of its inputs by Δ which is a pre-selected multiple of $1/(p-1)$. Subsequent sample points $X^{(i)}, i = 3, \dots, M+1$ are created in a similar way, namely from $X^{(i-1)}$ by perturbing one of its inputs which has not been perturbed before. After perturbing all inputs, we have $M+1$ sample points. A necessary condition to satisfy in generating the sample points is that all $X^{(i)}$ lie in the design space (for example, $[0, 1]^M$).

This process is captured in the following mathematical form:

$$B^* = (J_{M+1,1}X^{(1)} + (\Delta/2)[(2B - J_{M+1,M})D + J_{M+1,M}])P \quad (1)$$

where B^* is an $(M+1) \times M$ normalized design matrix (each row is one normalized sample point), $J_{m,n}$ is an $m \times n$ matrix of all 1's, D is an $M \times M$ diagonal matrix in which each diagonal element is either +1 or -1 with equal probability, $X^{(1)}$ is a row vector having the base sample, P is an $M \times M$ permutation matrix, and

$$B = \begin{bmatrix} 0 & 0 & 0 & \dots & 0 \\ 1 & 0 & 0 & \dots & 0 \\ 1 & 1 & 0 & \dots & 0 \\ 1 & 1 & 1 & \dots & 0 \\ \dots & \dots & \dots & \dots & \dots \\ 1 & 1 & 1 & 1 & 1 \end{bmatrix}.$$

To ensure this design creation process is a random selection from the distribution of elementary effect (to be defined later), the process uses three randomizations: (1) the base sample point is randomly selected, (2) the direction of the perturbation is random (that is, the creation of D), and (3) the choice of which input to perturb next is a randomized process (reflected by P). After B^* has been generated, this normalized sample has to be mapped onto the actual parameter ranges and distributions before running them through the simulations. This procedure is repeated $R-1$ times (for example, $R = 10$) to ensure enough regions in the design space has been explored.

After these sample points have been evaluated, the elementary effects for the inputs can then be calculated by:

$$d_{c(k)} = \frac{f(X^k) - f(X^{k-1})}{\Delta}, k = 2, \dots, M+1 \quad (2)$$

where $d_{c(k)}$ is defined as the elementary effect for input $c(k)$ (c maps k to its true input number). Note that since we randomly select which input to perturb next, the elementary effect computed using the k -th and $(k + 1)$ -th points in general is not the elementary effect for the k -th input which explains the $c(k)$ mapping.

Now that we have R elementary effects for each input (let's label them d_i^r for input i and replication r .) Morris proposed two sensitivity measures to analyze the data: μ which estimates the overall effect of each input on the output, and σ which estimates the higher order effects such as nonlinearity and interactions between inputs. The formulas for them are:

$$\mu_i = \frac{1}{R} \sum_{r=1}^R d_i^r, \quad \text{and} \quad \sigma_i = \sqrt{\frac{\sum_{r=1}^R (d_i^r - \mu_i)^2}{R}}, \quad (3)$$

respectively. Campolongo *et al.* [8] proposed an improved measure μ^* in place of μ where

$$\mu_i^* = \frac{1}{R} \sum_{r=1}^R |d_i^r|. \quad (4)$$

If μ_i^* is substantially different from zero, it indicates that input i has an important “overall” influence on the output. A large σ_i implies that input i has a nonlinear effect on the output, or there are interactions between input i and the other inputs.

2.3 Response Surface Methods

Response surface methodology (RSM) is a collection of statistical and mathematical techniques useful for developing, improving, and optimizing processes [5]. The original definition of RSM pertains to linear and polynomial regression analyses. We broaden the term RSM to include all function approximation methods. Provided that the model response Y is smooth enough, RSM can be very helpful in reducing the computational cost for uncertainty analysis. The idea is to create a set of sample points that are space-filling and use them to train a response surface model (or a function approximator). The choice of response surface methods for a given simulation model depends on the knowledge about the simulation model itself. If the model output is known to be a linear mapping of its uncertain inputs, then a first-order regression model suffices. If no such knowledge is available about the mapping, more general nonparametric models such as splines, neural network, or GP models may be more appropriate. Inference about new data points $(N + 1, \dots, N + k)$ from the already evaluated sample points $(1, \dots, N)$ can be expressed mathematically as:

$$P(Y_{N+k}|X_{N+k}) = F(X_1, \dots, X_N, Y_1, \dots, Y_N, \Phi)$$

which states that probability of the output being Y_{N+k} given X_{N+k} is a function of the evaluated sample of size N and the approximation method Φ .

Once a good response surface model has been constructed with sufficient accuracy (via rigorous validation and/or cross validation), subsequent analysis can rely on this response

surface model which is inexpensive to evaluate. This will facilitate the efficacy of the more quantitative analyses that require a large number of evaluations.

2.4 Variance Decomposition

So far the effort has been on identifying important parameters qualitatively. This section focuses on using variance to quantify input importance. The analysis techniques based on regression coefficients, correlation coefficients and their variants have limited applicability since they assume that the model is nearly linear or monotonic. Our attention is mainly on variance-based measures such as correlation ratio and Sobol'/Saltelli sensitivity indices which are less restrictive on the models. For applications with uncorrelated inputs, it is based on the full decomposition of the model variance $V(Y)$ (another notation for σ^2) into

$$V(Y) = \sum_i V_i + \sum_{i < j} V_{ij} + \sum_{i < j < k} V_{ijk} + \cdots + V_{12 \dots M} \quad (5)$$

where $V_i = V(E(Y|X_i))$, $V_{ij} = V(E(Y|X_i, X_j)) - V_i - V_j$, and so on. The total number of terms for M inputs is thus $2^M - 1$. In the present context, we are interested in the main effects (V_i), two-way interactions (V_{ij}) and total effect S_{T_i} .

The main effect analysis is due to McKay [2]. The essence of this analysis is the statistical measure called variance of condition expectation. Again, let $E(Y)$ and $V(Y)$ be the prediction mean and variance of an output variable Y , statisticians can tell us that

$$V(Y) = V(E(Y|X_i)) + E(V(Y|X_i)) \quad (6)$$

where X_i is the i -th input. Here the first term on the right hand side is the variance of the conditional expectation of Y , conditioned on X_i ; and the second term is an error or residual term.

We can extend the main effect analysis to two-way interaction studies (or second-order sensitivities) for uncorrelated inputs [8, 10]. In this case, we use the following relationship

$$V(Y) = V(E(Y|X_i, X_k)) + E(V(Y|X_i, X_k)) \quad (7)$$

where X_i and X_k are two distinct inputs under consideration. The first term on the right hand side is the variance of the conditional expectation of Y , conditioned on X_i and X_k . Again, the second term is the error or residual term measuring the estimated variance of Y by fixing X_i and X_k .

Finally, another measure that may be useful in the case of correlated inputs is the total sensitivity index S_{T_i} for input i which is defined as

$$S_{T_i} = V_i + \sum_{i \neq j} V_{ij} + \sum_{i \neq j, i \neq k} V_{ijk} + \cdots + V_{12 \dots M}. \quad (8)$$

All these measures can be computed using different numerical integration techniques.

2.5 Reliability/Failure Analysis

As a result of uncertainties in the model or input parameters, a finite probability may exist that a certain system will fail to deliver acceptable performance. Failure analysis is often needed to assess the reliability of the system. When there is a lack of information about the model behavior in the parameter space, this analysis will involve exploring the space thoroughly to identify failure regions and quantify the failure probability. This may be computationally intensive especially for high dimensional problems. When there is some prior information about the output distribution, Bayesian methods can be used to obtain the posterior distribution. Other smart methods such as the first order reliability method (FORM) are frequently used to reduce the computational cost.

We have also developed an adaptive sampling method to geometrically zoom into the threshold region. Our method employs a geometric adaptivity (as opposed to importance sampling in statistics) suitable for problems with medium dimensions (e.g. 2-10). The adaptive sampling is guided by formulating a utility function in the form of:

$$\{X_{n+1}, X_{n+2}, \dots, X_{n+m}\} = U(\{X_1, X_2, \dots, X_n\}, \{Y_1, X_2, \dots, Y_n\}, \theta, S)$$

where θ is the reliability threshold and S is the sampling strategy. Our method, as with many other methods, assumes that the model output is a continuous function of the uncertain inputs. In addition, smoothness of the function will help to accelerate the method. Users have to provide an initial sample size and the threshold. The algorithm divides the parameter space into regions, evaluates each region based on simulation outputs, and tags the regions that need to be refined. This process continues until the results meet a certain convergence criterion.

2.6 The PSUADE Software Package

To be able to perform designed simulation experiments like the ones used in uncertainty quantification, many detailed tasks such as setting up the test problem, negotiating the computational resources, extracting and processing the appropriate outputs for examination, packaging the outputs for visualization, applying the analysis tools, optimizing the responses, interpreting the results, etc. are involved. To simplify these tedious bookkeeping chores, we have developed PSUADE (short for Problem Solving environment for Uncertainty Analysis and Design Exploration), an integrated software environment, to facilitate the analysis. PSUADE supports a user-friendly interface via input and output filters. PSUADE provides a rich collection of sampling designs. Once a sampling design has been created, PSUADE systematically feeds the design points into parameter files and calls a user handler, which absorbs the sample data and inserts them into the model input files. The user handler then requests computational resource for the evaluation, waits for its completion, and extracts the output data from the model output files. This protocol allows all information exchange to be done via a user-written handler. There is no need to change the simulation source

code to accommodate the analysis, and it is sometimes called a “non-intrusive” interface. The results can be analyzed using PSUADE’s rich collection of response surface and analysis tools. PSUADE also creates ‘Matlab’ files for data visualization.

3 Numerical Experiments

3.1 Problem Definition

The original parameter distributions provided to us are lognormal distribution with some parameter correlations. In our preliminary numerical study we instead use uniform distributions with bounds at $\pm\sigma$ (one standard deviation) and no correlation for all parameters (Table 3.1). Each run takes about one minute on our Linux desktop.

Table 3: **Material parameters**

	Parameter	Distribution	Mean	range
Upper Cover Concrete	f_c	Uniform	27588.5	$\pm 0.2 * \text{Mean}$
	e_{c0}	Uniform	0.002	$\pm 0.2 * \text{Mean}$
	e_{cu}	Uniform	0.008	$\pm 0.2 * \text{Mean}$
Upper Core Concrete	f_c	Uniform	34485.6	$\pm 0.2 * \text{Mean}$
	f_{cu}	Uniform	20691.4	$\pm 0.2 * \text{Mean}$
	e_{c0}	Uniform	0.004	$\pm 0.2 * \text{Mean}$
	e_{cu}	Uniform	0.014	$\pm 0.2 * \text{Mean}$
Upper	E	Uniform	$2.0e8$	$\pm 0.033 * \text{Mean}$
Steel	S_y	Uniform	248200	$\pm 0.106 * \text{Mean}$
	Hkin	Uniform	1.613	$\pm 0.2 * \text{Mean}$
Foundation	E	Uniform	$2.0e7$	$\pm 0.2 * \text{Mean}$
Soil Layer #1	G	Uniform	54450	$\pm 0.3 * \text{Mean}$
	τ_{\max}	Uniform	33.0	$\pm 0.25 * \text{Mean}$
Soil Layer #2	G	Uniform	33800	$\pm 0.3 * \text{Mean}$
	τ_{\max}	Uniform	26.0	$\pm 0.25 * \text{Mean}$
Soil Layer #3	G	Uniform	61250	$\pm 0.3 * \text{Mean}$
	τ_{\max}	Uniform	35.0	$\pm 0.25 * \text{Mean}$
Soil Layer #4	G	Uniform	96800	$\pm 0.3 * \text{Mean}$
	τ_{\max}	Uniform	44.0	$\pm 0.25 * \text{Mean}$

3.2 Regression Analysis

We applied linear regression analysis to compute the standardized regression coefficients (SRC’s). We used an orthogonal array sample of size equal to 361. The results of this

analysis are valid if the responses are linear with respect to the input variables. For the 4 responses of interest, we obtained the adjusted R^2 of 0.92, 0.9, 0.93 and 0.77, respectively. The R^2 's indicate that linearity assumptions may be valid for response 1, 2, and 3 (the two IDR's and RDR), but inadequate for response 4 (MFA). We plot the SRC's in Figure 3.

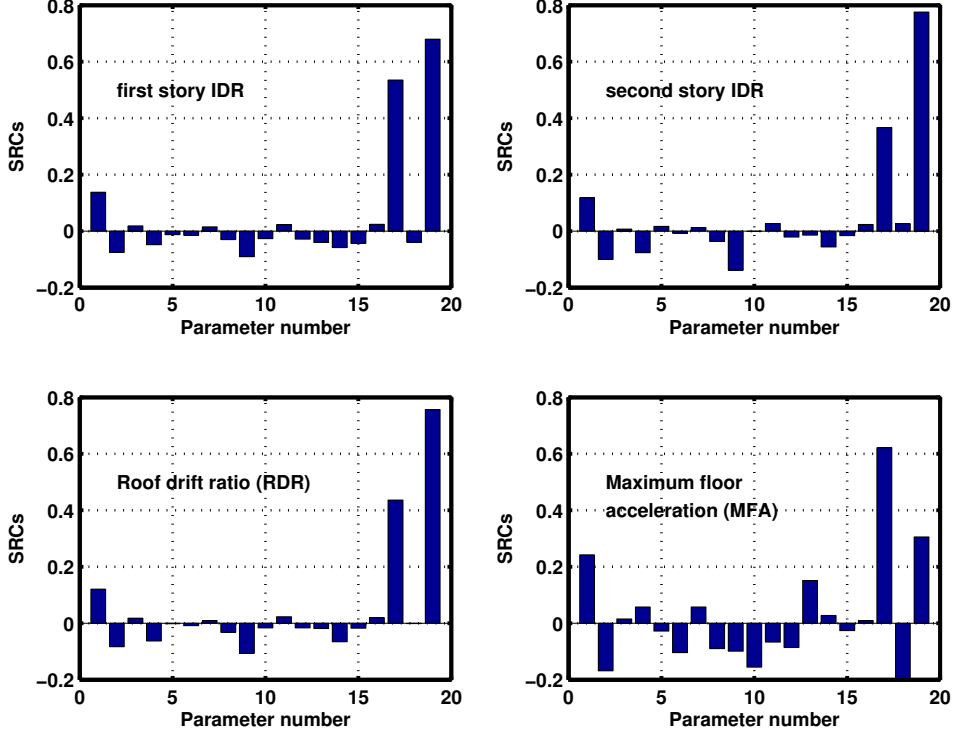


Figure 3: Standardized regression coefficients for the 4 responses of interest

Based on the above results, we have identified the following 5 parameters as important: $\tau_{\max,3}$ (parameter 17), $\tau_{\max,4}$ (19), σ_Y (9), f_c (1), and E_{c0} for the cover concrete (2).

3.3 Morris Screening Study

We applied screening analysis to identify qualitatively important parameters with respect to the responses of interest. We used the enhanced Morris sampling design with sample size $N = 600$ (usually $N = 200$ suffices, but we used larger N here since the simulation time is short). The normalized modified gradients due to the Morris analysis are shown in Figure 4. A large relative magnitude for a given input indicates its importance.

The conclusions from the Morris screening are that: for all the responses of interest, (1) the soil parameters $\tau_{\max,3}$ and $\tau_{\max,4}$ (parameters 17 and 19) are the most important; (2) the steel parameter σ_Y (parameter 9) is important; and (3) the upper structure cover parameters f_c and E_{c0} (parameter 1 and 2) are important. These agree well with results from regression analysis.

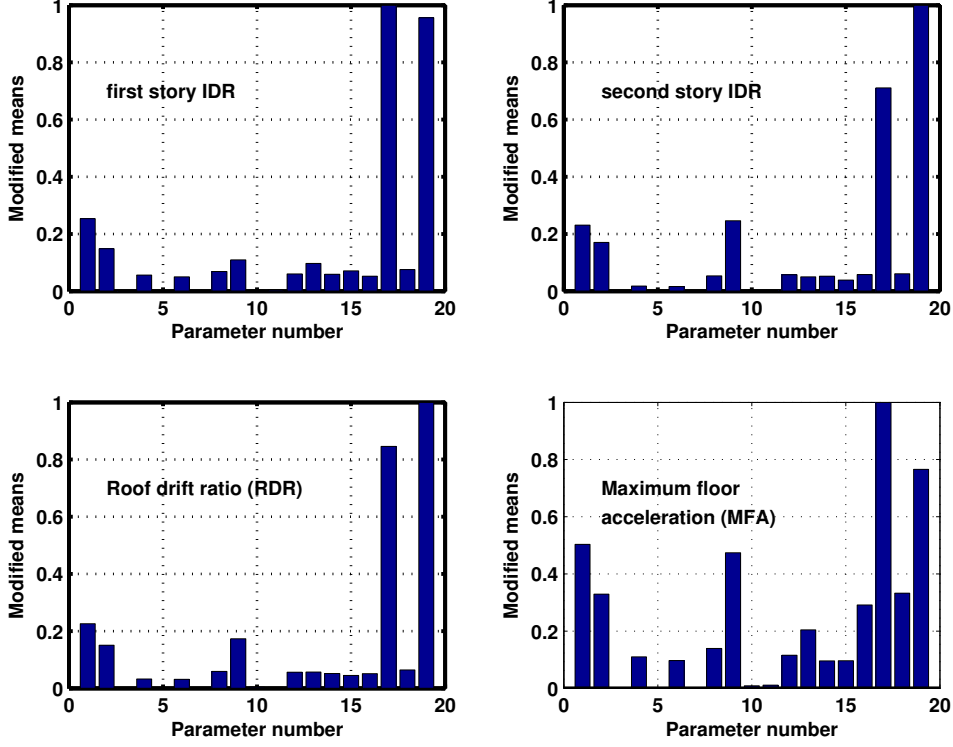


Figure 4: Parameter sensitivities for the 4 responses of interest

For more insights into the Morris analysis, we also present the Morris scatter plots (for individual gradients for each input) in Figure 5.

In Figure 5 we observe a wide spread of gradients for input 17 and 19 (the two τ_{\max} 's). For these two inputs, we further observe that, despite the large spreads of gradients, the spreads for triangles with same colors are relatively small (Triangles of same colors correspond to gradients with same values of the input). This means the spread is primarily due to the nonlinear effect of the individual inputs. We also applied variable resolution technique to study the screening sensitivities at a finer resolution ($p = 7$ and $N = 600$), and we found that the screening diagrams and scatter plots are essentially the same, implying that the current sampling resolution is adequate.

3.4 Response Surface Analysis

We applied a response surface methodology to the problem in the domain spanned by the ranges of the 5 parameters identified in the last section. To ensure a thorough exploration of the parameter space, we used a mixed design combining a 5-dimensional full factorial design of resolution 4 (to cover the corners and sides) together with about 800 (this number is arbitrary) runs of the LP- τ design. We used the full factorial design together with about 400 LP- τ runs as the training set; and withheld the remaining 400 LP- τ runs as the test set. We used the multivariate adaptive regression splines (MARS) [1] software library as the

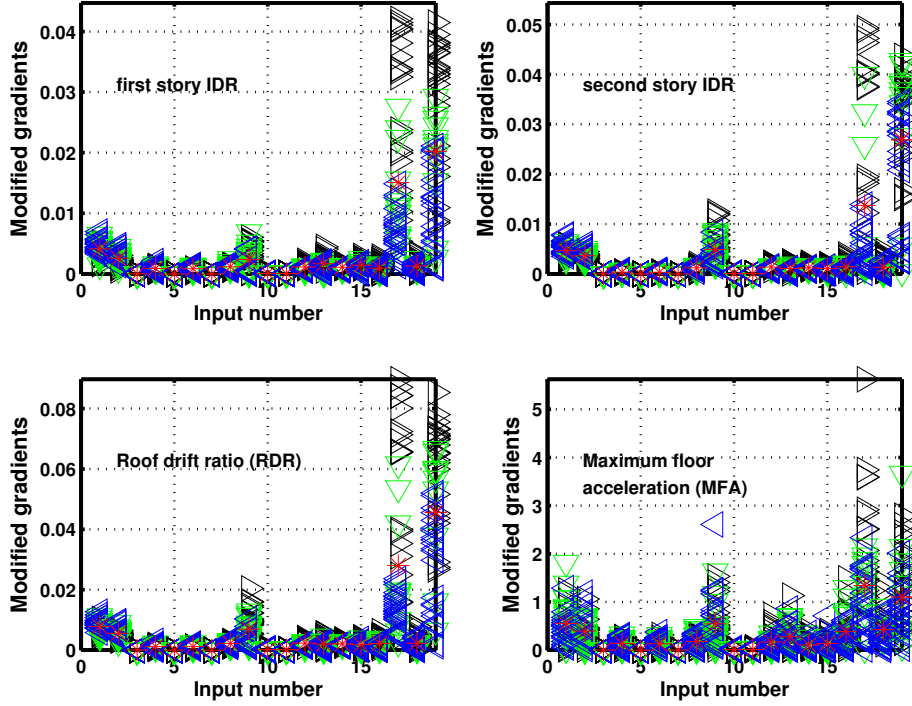


Figure 5: Morris scatter plots for the 4 responses of interest

function approximator. In Figure 6 we show the histogram of prediction error for the four different responses of interest. We observe that all except the last response give acceptable prediction errors. Therefore, our subsequent analysis will be limited to these three responses.

The response surface plots for the four responses of interest are given in Figure 7 to 10 as a function of the three most important parameters- τ_3 , τ_4 and cover f_c . We observe that the first three responses of interest vary much more significantly in the τ_3 (X) and τ_4 (Y) dimensions, but vary little in the cover f_c (Z) dimension demonstrating that τ_3 and τ_4 are the most important parameters. The response surface plot for the maximum floor acceleration appears to be nonsmooth, with a maximum prediction error of 60%.

3.5 Variance Decomposition Study

We performed variance decomposition on the response surfaces for the inter-story drifts and the roof drift ratio created in the last section. Using the approximate functions that are inexpensive to evaluate, we computed the first order sensitivity indices for the 5 parameters. For the current analysis we use uniform distributions and no correlation for all parameters. The breakdown of the total variance is given in Figure 11. We observe that τ_3 and τ_4 account for most of the output variances. Also, τ_3 by itself has a more significant effect on the first inter-story drift than the second. Note also that that the sums of all first

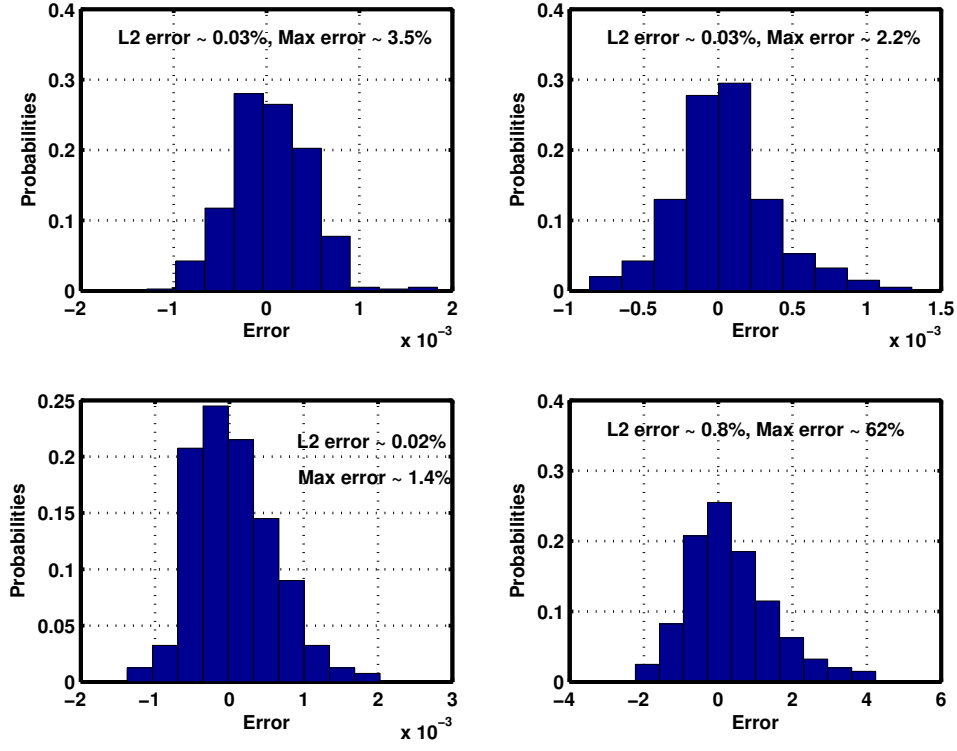


Figure 6: Histogram of prediction errors for the 4 responses of interest

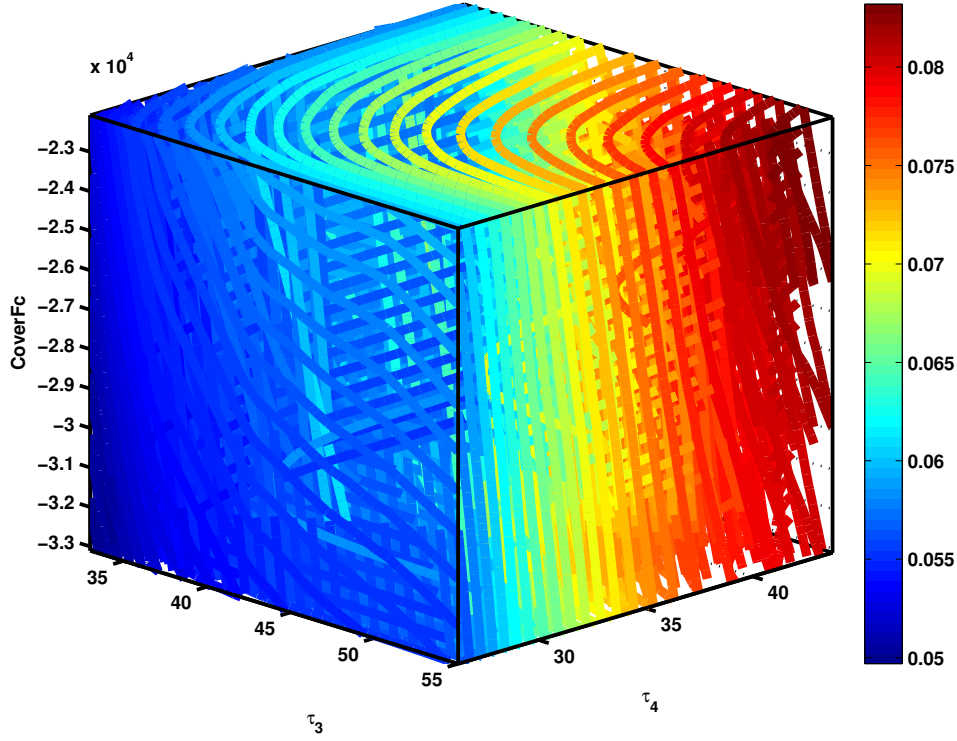


Figure 7: 3D response surface plot for maximum first inter-story drift

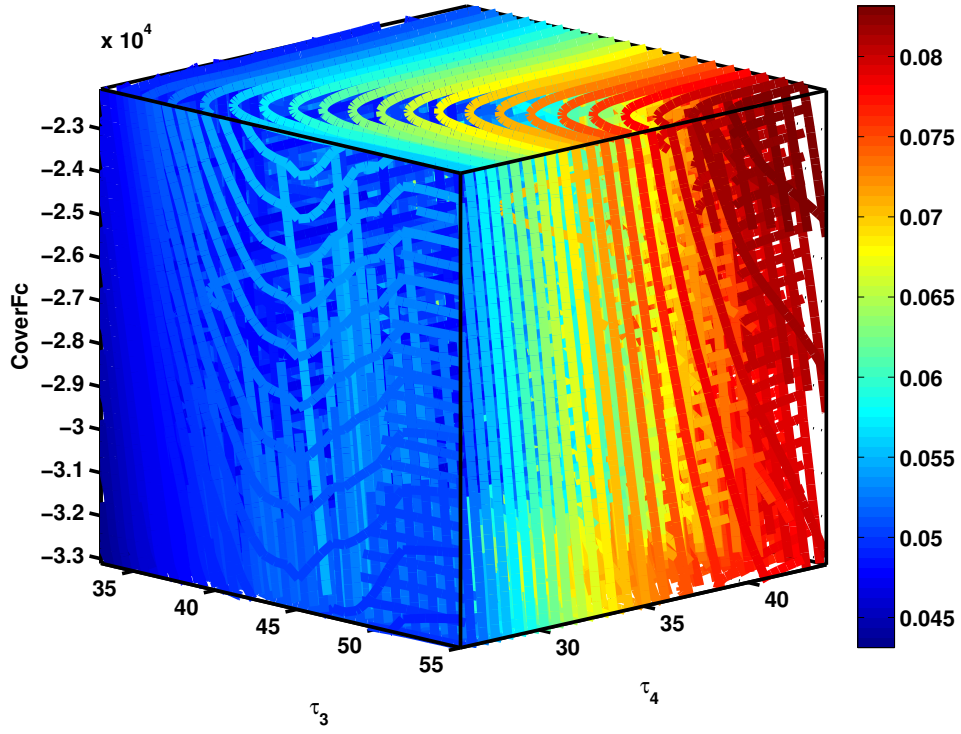


Figure 8: 3D response surface plot for maximum second inter-story drift

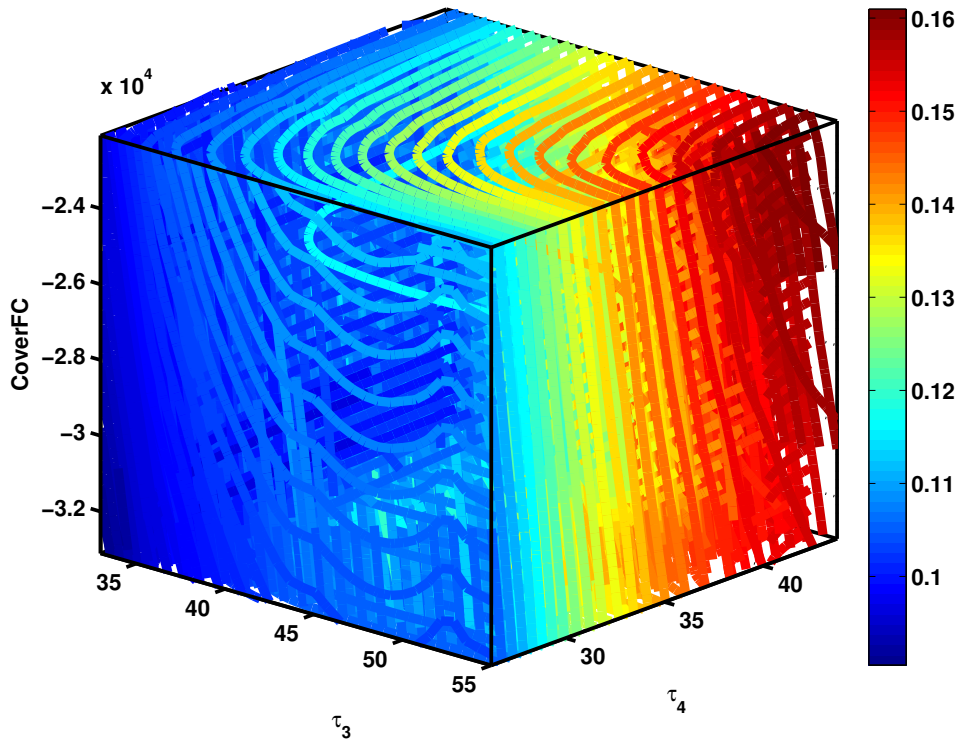


Figure 9: 3D response surface plot for maximum roof drift ratio

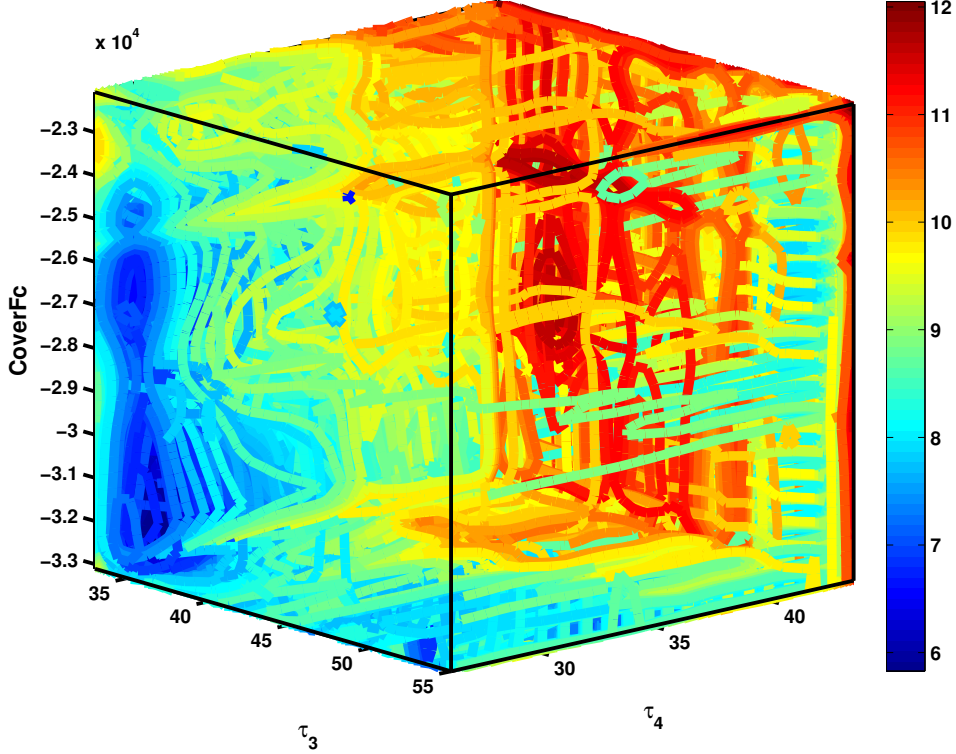


Figure 10: 3D response surface plot for maximum floor acceleration

order sensitivities are less than 1. This may be due to errors in the sensitivity indices as a result of finite sampling, and/or the presence of a small amount of interactions. Using multi-resolution analysis, we concluded that the error due to finite sampling is small (as indicated in the lower right plot in Figure 11, which shows the measure essentially converges for the 4 different resolutions. We also computed the second order sensitivity indices for pairs of parameters (Figure 12), which indicated that the remaining variance is mainly due to interaction between τ_3 (parameter 4) and τ_4 (parameter 5).

The total sensitivity indices for the 5 parameters are given in Table 3.5.

Table 4: **Total sensitivity indices for inter-story and roof drifts**

Input	1st story drift	2nd story drift	roof drift
1	0.028	0.023	0.022
2	0.014	0.015	0.013
3	0.012	0.025	0.012
4	0.424	0.275	0.320
5	0.576	0.761	0.705

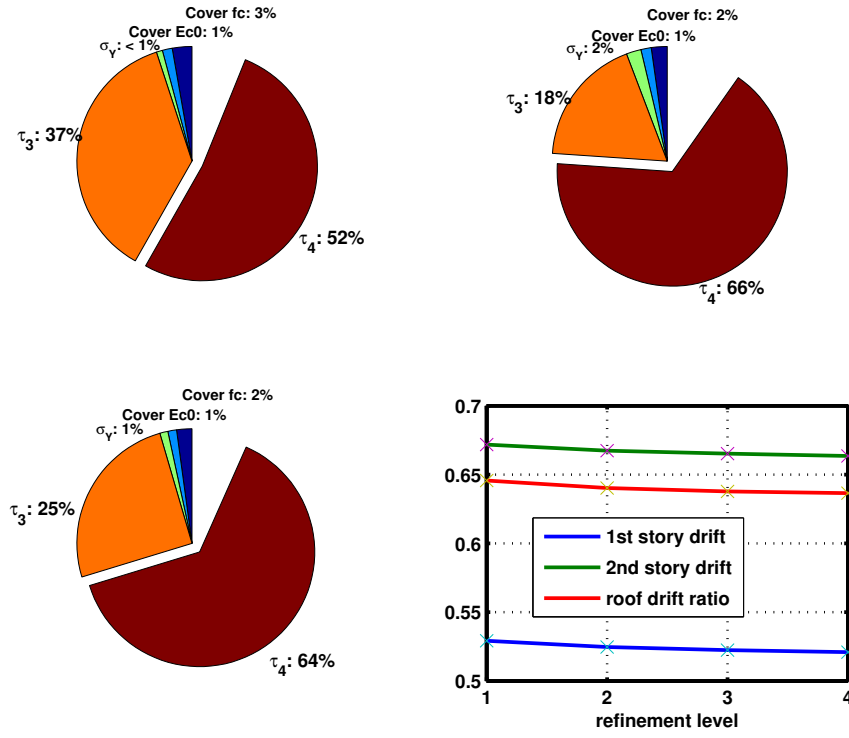


Figure 11: First order sensitivity indices for : (upper left) first inter-story drift, (upper right) second inter-story drift, (lower left) roof drift ratio, (lower right) convergence of $VCE(\tau_4)$

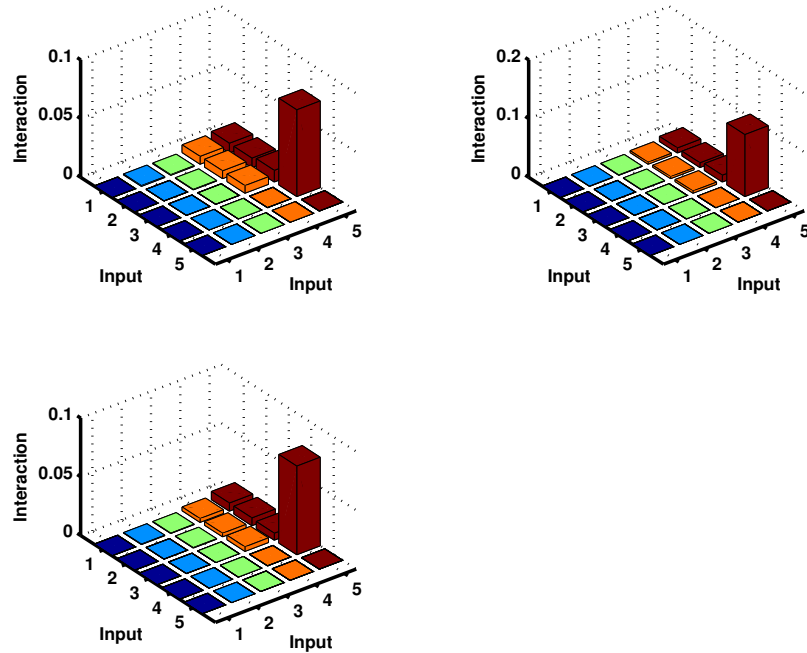


Figure 12: Second order sensitivity indices for : (upper left) first inter-story drift, (upper right) second inter-story drift, (lower left) roof drift ratio

3.6 Bayesian Sensitivity Study

The regression analysis above suggests that the first 3 responses may be smooth functions of the uncertain parameters. So, in addition to applying the multi-step sensitivity analysis, we also performed direct variance decomposition on the 19-parameter problem. We used the same sample design as in regression analysis, namely, orthogonal array with sample size 361 and strength 2. We used the sample input and output data to create a response function using Gaussian process. Unfortunately, the two Gaussian process software packages that we selected, Mackay's Tpros ([3]) and Rasmunssen's GP, complained about encountering indefinite covariance matrices. We thus resorted to using MARS ([1]) to fit the data. We performed variance decompositions on the MARS-based response functions, the result of which are given in Table 3.6.

Table 5: **First sensitivity indices for inter-story and roof drifts**

Input	1st story drift		2nd story drift		roof drift	
	VCE (A)	VCE (B)	VCE (A)	VCE (B)	VCE (A)	VCE (B)
1	0.028	0.028	0.022	0.023	0.022	0.021
2	0.014	0.011	0.015	0.014	0.012	0.010
3	—	0.000	—	0.000	—	0.000
4	—	0.002	—	0.000	—	0.001
5	—	0.000	—	0.000	—	0.000
6	—	0.001	—	0.000	—	0.000
7	—	0.000	—	0.000	—	0.000
8	—	0.003	—	0.002	—	0.002
9	0.009	0.008	0.021	0.021	0.011	0.012
10	—	0.000	—	0.000	—	0.000
11	—	0.000	—	0.000	—	0.000
12	—	0.003	—	0.002	—	0.001
13	—	0.003	—	0.000	—	0.001
14	—	0.002	—	0.001	—	0.002
15	—	0.003	—	0.001	—	0.001
16	—	0.000	—	0.000	—	0.000
17	0.368	0.380	0.182	0.190	0.252	0.257
18	—	0.000	—	0.001	—	0.000
19	0.521	0.502	0.663	0.665	0.637	0.636
'—' measures not computed						
'VCE(A) : first order sensitivities from multi-step method						
'VCE(B) : first order sensitivities from direct method						

In the tables we also included the first order sensitivity indices computed from the multi-step approach. Here we observe that the results from both approaches match quite well. We attribute this to the highly smooth nature of the three model responses under study.

3.7 Uncertainty Analysis

We have shown that the response surfaces for the first three responses of interest are adequate. In this section we use the response surfaces to compute some uncertainty measures. To compute the basic statistics we probed the response surfaces with Latin hypercube samples of size 200000. The histograms showing output distributions are given in Figure 13. The statistical numbers are given in Table 3.7 (The kurtoses have not been offset.)

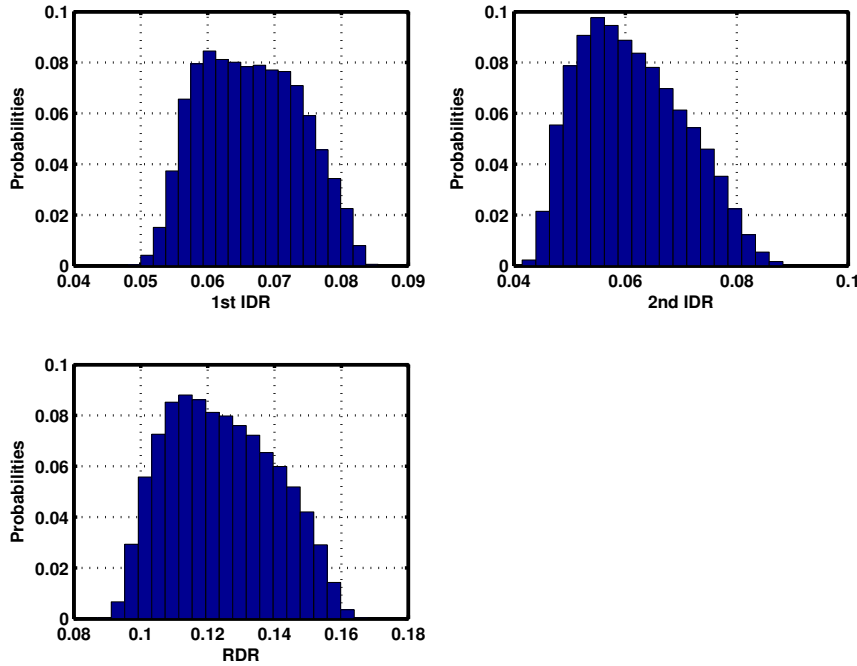


Figure 13: Histograms for the uncertainties of 3 responses of interest

3.8 Reliability Analysis

To demonstrate our adaptive sampling capability for reliability analysis, we applied our tool to the study of roof drift ratio. We artificially prescribed the reliability threshold to be 0.15 and observed our algorithm zooming in around the threshold region. Our convergence criterion is such that two consecutive refinements give reliability measures that differ by less than 0.1%. Our algorithm used 7 levels of adaptive refinement with a total sample size of 1434 giving a final reliability of 93.4%. From our experiences with other problems, it would have taken $> 10X$ more sample points if non-adaptive sampling is used.

Table 6: **Uncertainty results for the three responses of interest**

Measure	1st IDR	2nd IDR	RDR
mean	0.0664	0.0613	0.1240
standard deviation	0.0073	0.0093	0.0159
skewness	0.131	0.345	0.204
kurtosis	2.10	2.31	2.12
IDR - maximum inter-story drift ratio RDR - maximum roof drift ratio			

Table 7: **Reliability analysis data for roof drift ratio**

Level	nSamples	Reliability (%)
0	50	98.00
1	20	97.00
2	32	95.00
3	59	93.75
4	108	94.13
5	197	93.44
6	356	93.47
7	612	93.42

4 Summary

This document shows how to perform global sensitivity analysis and failure analysis for scientific or engineering models. Different techniques may be viable depending on the nature of the model outputs. Even though the regression and Bayesian-type analysis give accurate sensitivity results for this high-dimensional problem, we recommend to validate the direct approach with the multi-step approach, since the direct approach assumes highly smooth functions. Screening methods are useful not only in sensitivity analysis, but also in reducing the number of parameters for other analysis such as failure analysis and optimization. Response surface methods are essential in reducing the overall computational cost. The essence of response surface methods are to fill in the space between the evaluated sample data making certain continuity and smoothness assumptions. Variance decomposition is a useful technique to attribute the output variability to individual inputs. Finally, we showed that adaptive or importance sampling can be useful in reducing the cost of reliability analysis.

The current study emphasizes on robust uncertainty and sensitivity analyses. Future work will move on to the 3D soil-foundation-structure interaction problem, which takes

about an hour per run. For that problem, we will concern more about efficiency. We plan to employ intelligent sampling to perform response surface and other statistical analyses.

Acknowledgement : The author would like to thank Professor Joel Conte and Quan Gu from UCSD for providing the 2D SFSI model and the help in using their OpenSees code, and Radu Serban for setting up OpenSees on my LLNL desktop.

References

- [1] J. H. Friedman, *Multivariate adaptive regression splines*, *Annals of Statistics* 19.1, 1-141, 1991.
- [2] M. D. McKay, *Evaluating Prediction Uncertainty*, Los Alamos National Laboratory Technical Report NUREG/CR-6311, LA-12915-MS.
- [3] M. Gibbs and D. Mackay, *Efficient Implementation of Gaussian Processes*, A report available from Cambridge Gaussian Process website.
- [4] M. D. Morris, *Factorial Sampling Plans for Preliminary Computational Experiments*, *Technometrics*, 21(2), pp. 239-245, 1991.
- [5] R. H. Myers and D. C. Montgomery, *Response Surface Methodology*, Second Edition, Wiley Series in Probability and Statistics, 2002.
- [6] J. E. Oakley and A. O'Hagan, *Probabilistic Sensitivity Analysis of Complex Models: a Bayesian approach*, *J. R. Statist. Soc. B* (2004), 66, Part 3, pp. 751-769.
- [7] C. E. Rasmussen, *Evaluation of Gaussian processes and other methods for non-linear regression*, PhD thesis, University of Toronto, 1996.
- [8] A. Saltelli, K. Chan, E. M. Scott (editors), *Sensitivity Analysis*, Wiley Series in Probability and Statistics, 2000.
- [9] C. Tong and F. Graziani, *A Global Sensitivity analysis Methodology for Multi-physics Applications*, LLNL report UCRL-TR-227800, 2007.
- [10] C. Tong, *Toward a More Robust Variance-based Global Sensitivity Analysis of Model Outputs*, LLNL report UCRL-TR-235561, 2007.
- [11] C. Tong, *The PSUADE Software Package Version 1.0*, LLNL code release UCRL-CODE-235523, 2007.